Meteoritics & Planetary Science 40, Nr 8, 1149–1157 (2005)
Abstract available online at http://meteoritics.org

An appraisal of the Serra da Cangalha impact structure using the Euler deconvolution method

A. Adekunle ADEPELUMI[1*], Jean M. FLEXOR[2], and Sergio L. FONTES[2]

[1]Department of Geology, Obafemi Awolowo University, Ile-Ife, Osun State, Nigéria
[2]Departamento de Geofísica, Observatório Nacional, Rua Jose Cristino 77, CEP 20921–400, São Cristóvão, Rio de Janeiro, Brazil
[*]Corresponding author. E-mail: adepelumi@yahoo.co.uk

(Received 18 August 2003; revision accepted 25 May 2005)

Abstract–The applicability of the Euler deconvolution method in imaging impact crater structure vis-à-vis delineation of source depth of the circular magnetic anomaly and/or basement depth beneath the crater is addressed in this paper. The efficacy of the method has been evaluated using the aeromagnetic data obtained over the Serra da Cangalha impact crater, northeastern Brazil. The analyses of the data have provided characteristic Euler deconvolution signatures and structural indices associated with impact craters. Also, through the interpretation of the computed Euler solutions, our understanding of the structural features present around the impact structure has been enhanced.

The Euler solutions obtained indicate shallow magnetic sources that are interpreted as possibly post-impact faults and a circular structure. The depth of these magnetic sources varies between 0.8 and 2.5 km, while the Precambrian basement depth was found at ~1.5 km. This is in good agreement with the estimates of the Precambrian basement depth of about 1.1 km, calculated using aeromagnetic data. The reliability of the depth solutions obtained through the implementation of the Euler method was confirmed through the use of the existing information available in the area and the result of previous studies. We find that the Euler depth solutions obtained in this study are consistent with the results obtained using other methods.

INTRODUCTION

For a long time, meteorite impacts were lackadaisically regarded as an interesting phenomenon in the spectrum of geological processes affecting the Earth but not as an important phenomenon. Change in this perspective occurred over the past 30 years as a result of space exploration, which produced compelling evidence that all planetary surfaces are cratered as a result of impacts of interplanetary bodies. Today, studies of meteorite impacts have become the subject of prime interest worldwide, as the scientific communities have come to realize the importance of impacts for global environmental devastation and the mass extinction of animal and plant species (Tappan 1982).

Earth is known to be geologically active, resulting in the obliteration of most crater scar imprints through erosion, weathering, and tectonic activity (Pilkington and Grieve 1992). By the end of 2004, only about 172 impact craters have been identified on Earth (see http://www.unb.ca/impactdatabase/index.html). Several more are found each year. In Brazil alone, there are currently five established impact structures: Araguainha, Serra da Cangalha (the subject of this paper), Riachão, Vargeão, and Vista Alegre. Another eight probable ones—Colônia, São Miguel do Tapuio, Cerro Jarau, Piratininga, Santa Marta, Inajah, Curuçá, and Aimorés—are still being investigated (Crósta 1987; Pilkington and Grieve 1992). These structures range in size from about 4 to 40 km.

With the help of ERTS-1 (now LANDSAT) satellite images, Dietz and French (1973) first found and reported the Serra da Cangalha crater as a probable astrobleme mainly due to its circular shape. Serra da Cangalha is known as the second largest impact crater in Brazil (Crósta 1987), having a diameter of 12 km, estimated from satellite imagery. This impact structure is located at 46°52′W and 8°05′S in northeast Brazil (Fig. 1). The structure is characterized by a distinct uplifted annular trough and a prominent circular central ring with a diameter of 5 km and a height of about 300 m above the surrounding terrains (Adepelumi et al. 2005).

The use of Euler deconvolution as an interpretation tool to determine source location of potential fields' anomalies is well established (Mushayandebvu et al. 2004). The method

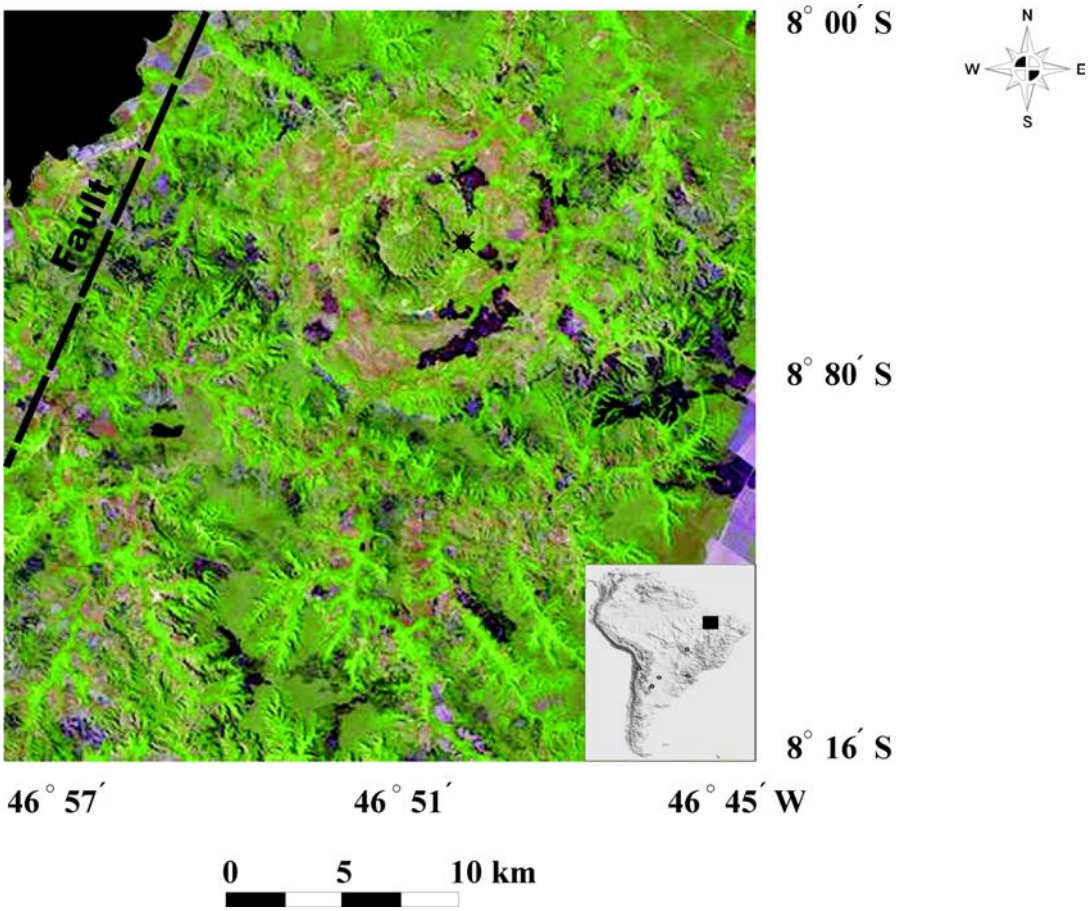

Fig. 1. A LANDSAT image of the Serra da Cangalha impact crater region. The location of the three shallow boreholes drilled by Geological Survey of Brazil is indicated close to the center of the crater. Also, the fault superimposed on the image was extracted from the geological map of the area.

has long been used in automatic aeromagnetic interpretations because it requires no prior knowledge of the source magnetization direction and assumes no particular interpretation models. Various authors have used the Euler method to image craters; examples are Charlevoix, Canada (Keating 1998) and the Bangui anomaly, central Africa (Ravat et al. 2002a). The objective of this paper is to apply the Euler method to aeromagnetic data acquired over the Serra da Cangalha impact crater to estimate the depth of the magnetic anomaly and the depth to the Precambrian basement beneath the crater and to map the structural features associated with the crater.

GEOLOGICAL AND HYDROLOGICAL SETTINGS

The Serra da Cangalha structure was formed in the intracratonic Parnaíba basin of northeastern Brazil. Local stratigraphy comprises upper Silurian to Cretaceous sedimentary rocks roughly 1200 m thick (Góes and Feijó 1994; Adepelumi et al. 2005). The youngest sedimentary formation, Pedra de Fogo, lies over the Piaui formation, followed by the Poti and the Longá formations. The oldest sedimentary rock in the area is the Cabeças formation. The upper Permian Pedra do Fogo formation (290–255 Ma) consists of poorly sorted silty-sandstone having conspicuous beds of white chart nodules. The Permian/Carboniferous Piauí formation (323–290 Ma) consists of fine-medium grained grey-whitish sandstones that gradually graded to conglomerate with intercalation of reddish carbonaceous shales and whitish limestone. Rocks of this formation are found in the impact structure between the outer edge of the inner ring and the outer ring, herein referred to as the crater rim or external part of the crater. The Poti formation, Mississippian in age (354–323 Ma), is composed of dark shales with small amounts of fine bituminous silt and a thin mica lamination. The upper Devonian-Mississippian (365–354 Ma) sedimentary sequence locally called the Longá formation was deposited in a tidal, regressive phase environment. Finally, the Cabeças formation is middle Devonian (385–354 Ma) in age. The Poti and Longá formations occur within the inner ring (central part) of the crater.

Mapping studies by McHone (1986) and Dietz and French (1973) show structural disturbance of the sediments

Table 1. Relationship between structural index (η), type of magnetic model, and position of the calculated depth (modified after Hsu 2002).

Structural index (η)	Type of magnetic model	Position of Euler depth
0.0	Contact with large depth extent	At top and edge
0.5	Contact with small depth extent	–
1.0	Thin prism with large depth	At top and center, or at edge and half throw
2.0	Vertical or horizontal cylinder	At center
3.0	Sphere	At center

found at the center of the crater. They attribute the cause of this disturbance to structural collapse and near-surface fracturing. Furthermore, in the inner ring, there are severely deformed, steeply dipping (>60°) sedimentary structural patterns. More recently, Adepelumi et al. (2005) evaluated the magnetotelluric data acquired across the crater and suggested that impact-induced structural deformation is limited to a 2 km depth. Further evidence from the Geological Survey of Brazil (CPRM 1972) shows that the annular inner depression of the crater is filled with impact-derived materials made up of very minute allochthonous monomictic breccias and minor impact melt bodies.

Field and microscopic evidence support a meteoritic origin for the structure, and the occurrence of shock metamorphism features like shatter cones in quartzite boulders of a conglomerate were found at the base of the Poti formation (Beatty 1980), while McHone (1986) reports on shock breccia, lamellae, impact melt, rhombic fractures and joints, unusual micro-fracturing of quartz grains, shock-induced optical planar elements ($10\bar{1}2$ and $10\bar{1}3$), and microspherules. The assigned age of the impact crater structure, most probably Triassic or post-Triassic (<220 Ma), was estimated purely on the regional stratigraphy found at the impact site, while blocks of fossil wood found in the crest of the central uplift suggest that the impact occurred on land (McHone 1986). Geologic evidence at the crater site rule out an endogenic origin due to igneous intrusion or salt diapir because igneous rocks are entirely absent in this region and the sediments underlying the structure do not contain any significant carbonate or salt units. McHone (1986) interpreted the formation of the entire central depression area of the crater to be mainly due to fluvial erosion rather then the original explosion crater morphology. Surface drainage morphological features extracted from LANDSAT imagery (Fig. 1) include well-developed annular drainage that interrupts the radial and dendritic drainage patterns common at the Serra de Cangalha site. Active streams that breach the north rim of the inner mountain ring drain the entire structure. It then merges with an annular drainage system in the ring trough and flows out of the structure to the northwest. The horseshoe shape of the inner-ring is due to the differential weathering and erosion of the alternating soft and resistant sedimentary strata. The least resistant sediments are the Devonian shale in the central crater and the Pennsylvanian silt-and-argillite layers in the depressed ring trough. These rocks are the most porous rocks in this region, and they contain near-surface groundwater. The compact sandstones, silicified fissures, and silica-rich strata are the most resistant to erosion. According to McHone (1986), the Serra de Cangalha site has undergone very intense erosion and weathering, losing over 350 m of the originally overlying sedimentary strata.

METHODOLOGY

The Euler deconvolution method is a quasi-automated interpretation method often used for estimating depths and delineating boundaries of anomalous bodies (Keating and Pilkington 2004; Cooper 2002). Application of the method to the derivatives of potential field data to estimate depths has been shown to be effective and useful (Ravat et al. 2002b; Hsu 2002). In particular, this shows that the Euler method can be used successfully to estimate location and depth of magnetic anomalies.

The most critical parameter in the Euler deconvolution is the structural index, η (Thompson 1982). This is a homogeneity factor relating the magnetic field and its gradient components to the location of the source (Table 1). Essentially, η measures the rate of change of the fields with distance from the source (fall-off-rate) and is directly related to the source dimensions. Therefore, by estimating η, we can provide information on the geometry and depth of the magnetic sources. A poor choice of the structural index has been shown to cause a diffuse solution of source locations and serious biases in depth estimation (Hsu 2002; Keating and Pilkington 2004). Both Thompson (1982) and Reid et al. (1990) suggested that a correct η gives the tightest clustering of the Euler solutions around the geologic structure of interest. For magnetic data, physically plausible η values range from 0 to 3. The magnetic field of a point dipole falls off as the inverse cube, giving an index of 3, while an effective vertical line source such as a narrow, vertical pipe gives rise to an inverse square field fall-off and an index of 2. Values less than zero imply a field strength that increases with distance from the source (and is infinite at infinity) (Table 1).

The magnetic field due to a point source such as a pole or dipole at a position (x_o, y_o, z_o) has the form (Durrheim and Cooper 1998):

$$\Delta T(x, y) = f([x - x_o], [y - y_o], z_o) \quad (1)$$

$$f(x, y, z) = M/r^{\eta} \quad (2)$$

where r is distance, $(x^2 + y^2 + z^2)^{½}$, and M is proportional to

magnetization. A function (f) is said to be homogeneous of degree n if it satisfies Euler's equation given as:

$$\begin{bmatrix} \frac{\partial T}{\partial x_1} & \frac{\partial T}{\partial y_1} & \frac{\partial T}{\partial z_1} & \eta \\ \vdots & \vdots & \vdots & \vdots \\ \vdots & \vdots & \vdots & \vdots \\ \frac{\partial T}{\partial x_n} & \frac{\partial T}{\partial y_n} & \frac{\partial T}{\partial z_n} & \eta \end{bmatrix} \times \begin{bmatrix} x_o \\ y_o \\ z_o \\ B \end{bmatrix} = \begin{bmatrix} x_1 \frac{\partial T}{\partial x_1} + y_1 \frac{\partial T}{\partial y_1} + z_1 \frac{\partial T}{\partial z_1} + \eta T \\ \vdots \\ \vdots \\ x_n \frac{\partial T}{\partial x_n} + y_n \frac{\partial T}{\partial y_n} + z_n \frac{\partial T}{\partial z_n} + \eta T \end{bmatrix} \quad (3)$$

where (x_o, y_o, z_o) is the source position, the total field (T) of which is detected at (x_1, y_1, z_1), with a regional field value (B). In this study, we use the program EULDEP, which performs the Euler deconvolution of magnetic data in two-dimensions (2-D), by assuming that the magnetic field is symmetric transverse to the profile so that $\partial \Delta T / \partial y = 0$ (Durrheim and Cooper 1998). The total magnetic field is given by the sum of the regional field and the anomaly due to a point source. Since the total magnetic fields are known, the program calculates the gradients ($\partial T / \partial x$, $\partial T / \partial y$, and $\partial T / \partial z$) associated with it. A system of least-square inversion then determines the anomaly position x_o, depth z_o, and base level B for a specific magnetic source.

The interpretation of potential methods for data analysis is inherently ambiguous, and every interpretation method has its own disadvantages and limits. The pitfalls and drawbacks associated with the Euler deconvolution method are few compared to other geophysical interpretation techniques. Some of these limitations are highlighted as follows: 1) only estimates about the geometrical characteristics of the anomaly sources are given, and no information about their physical properties can be obtained; 2) the presence of noise in the magnetic data will distort the shape of any existing magnetic anomalies present making it look like an undisturbed magnetic source. Therefore, it is imperative to remove noise from the data before interpretation using low pass filter. If this is not done, all depth estimates obtained will be erroneous and misleading (Durrheim and Cooper 1998); 3) the depth estimates from the Euler method are generally thought to be uncertain; hence, the estimated depths solutions must be integrated with other geophysical methods; 4) the absence of susceptibility and dip estimates (Reid et al. 1990); 5) if a window size is used that is large enough to encompass two or more neighboring anomalies, they will be incorrectly considered as one anomaly. However, a range of window sizes are used, and the smaller sizes will resolve the individual anomalies better and produce a more accurate source location (Cooper 2002); 6) in practice, Euler's homogeneity equation is valid only for bodies of arbitrary shape. For such geometries, the structural index (SI) is an integer, as bodies that do not fall within the range of the stipulated SI values are not accounted for; and 7) unstable and dispersed Euler solutions will be obtained when a wrong choice of structural index is made.

Aeromagnetic Data and Data Processing

The aeromagnetic data over the survey area were obtained at a constant terrain clearance of 150 m. Profiles were measured in the N–S direction, perpendicular to the observed regional strike, at magnetic declination and inclinations 17.8° and 0.6°, respectively. The profiles were spaced 4 km apart and tie lines were flown at a spacing of 27 km in an E–W direction. Data were subjected to some basic data filtering techniques before applying the Euler deconvolution method. They allowed us to remove the regional earth's magnetic field (IGRF) and the diurnal variations. The resulting data represents the residual magnetic anomaly, which was gridded and contoured using the OASIS montaj software for 3-D data interpretation (Fig. 3), while the data along the profiles were extracted for 2-D interpretation purposes. During this procedure, the improved Euler deconvolution algorithm incorporates the calculation of vertical gradients in frequency domain. Therefore, the vertical gradients were calculated as to minimize noise (see Cooper 2002; Gunn 1975). The Euler solutions computed have been obtained using the vertical gradient as the main data set.

For the 2-D data interpretation, depth estimation was made along the three flight lines D–D', E–E', and F–F' in Fig. 3. Euler solutions were obtained for structural index values of 0.5, 1.0, 1.5, 2.0, and 3.0 (Fig. 3). For the grid data, we show the result for $\eta = 2.0$ and 3.0 in Fig. 4, since line and point dipole sources are appropriate for estimating the depth of a structure with circular geometry. Depth limits, obtained through a magnetotelluric method and downward continuation of the aeromagnetic data by Adepelumi et al. (2005), and well logs by Góes and Feijó (1994) have been used here to constrain the Euler results obtained. Subsequently, solutions that fall outside these ranges have been rejected. Vertical gradient maxima and horizontal gradient minima have been used to delimit the horizontal extent of the crater (Ravat et al. 2002b; Grauch and Cordell 1987).

DISCUSSION OF RESULTS

The Serra de Cangalha structure is characterized by a distinct central low positive magnetic anomaly having a relief of 33 nT, surrounded by sub-circular highs from the northern and southern sides (Fig. 2). The widely spaced profiles do not allow us to obtain a high resolution image of the crater. However, Fig. 2 suggests that a NE–SW regional field dominates the crater region.

The Euler solutions obtained along profiles D–D', E–E', and F–F' are shown in Figs. 3a, 3b, and 3c, respectively. The figures show a distinct clustering of solutions at the crater edges. All three profile results exhibit very similar patterns

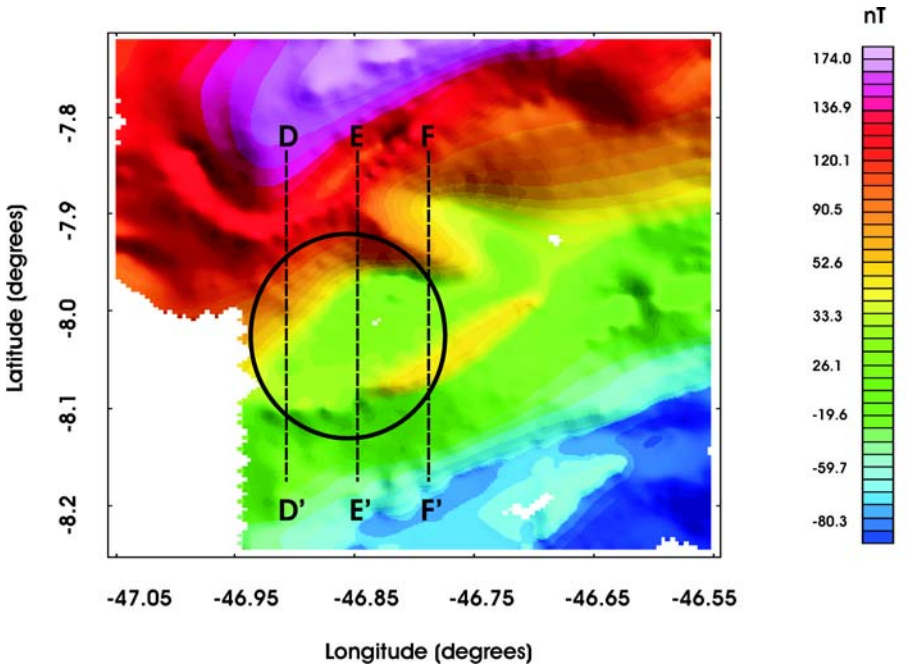

Fig. 2. An aeromagnetic map of Serra da Cangalha (residual fields) showing the locations of the three profiles (across the crater) used for the 2-D Euler deconvolution. The data shown in this map was obtained after subtracting the main magnetic fields of 27350 nT from the total magnetic field data. The central ring shows the impact crater region.

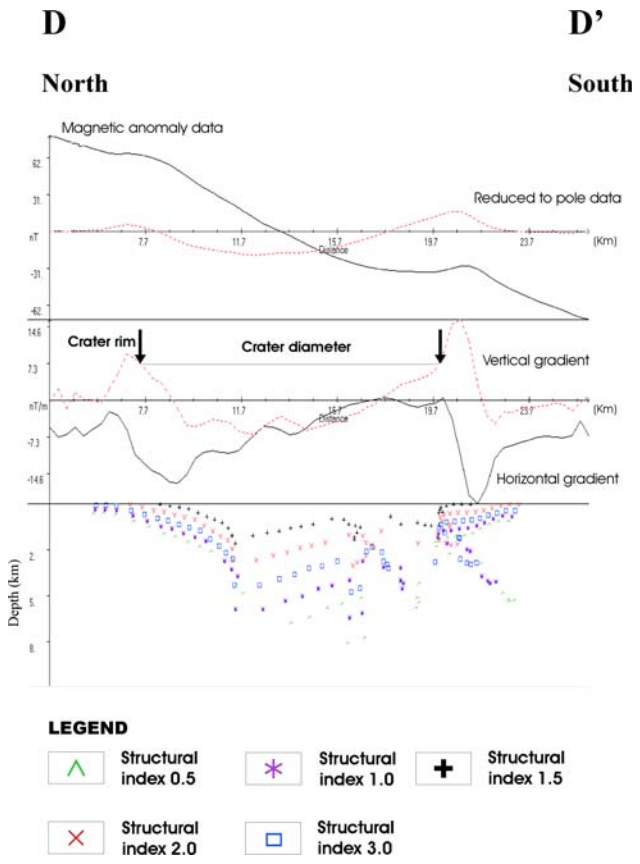

Fig. 3a. Results of Euler deconvolution of vertical derivative data along profile D–D'.

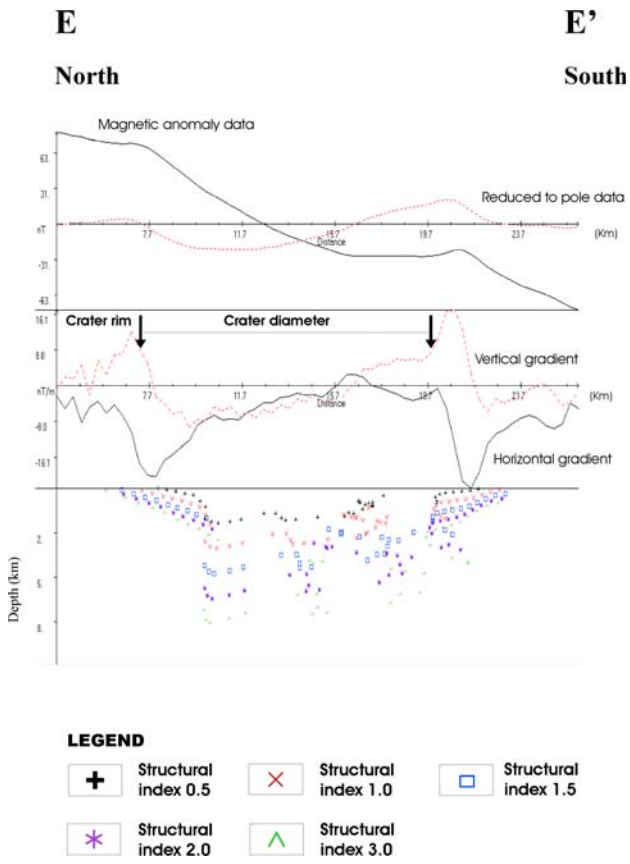

Fig. 3b. Results of Euler deconvolution of vertical derivative data along profile E–E'.

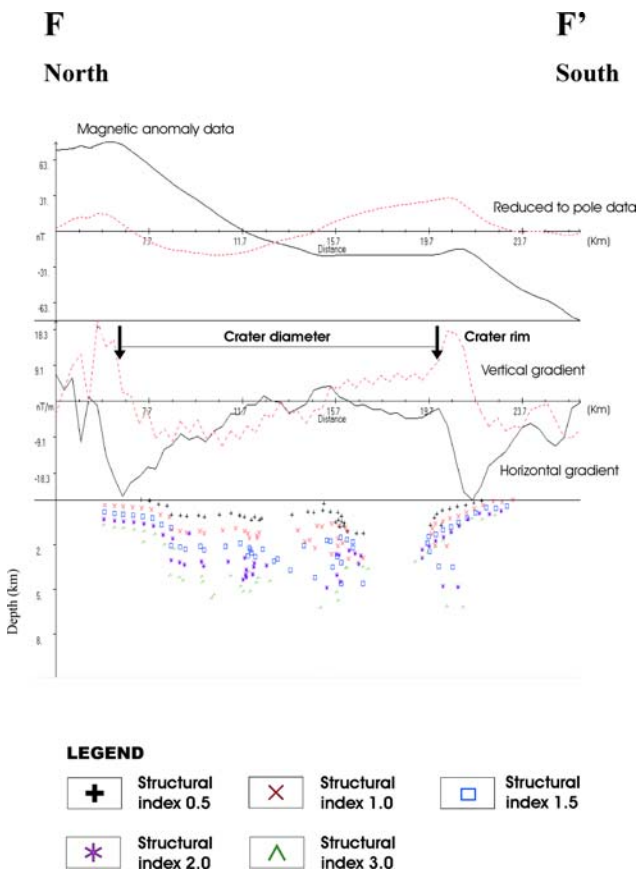

Fig. 3c. Results of Euler deconvolution of vertical derivative data along profile F–F'.

and trends. The rims of the Serra da Cangalha crater are well-delineated between the distance 7.7 and 19.7 km on profiles D–D' (Fig. 3a) and E–E' (Fig. 3b) and between 6.7 to 20.2 km on profile F–F' (Fig. 3c). Horizontal and vertical gradient maxima and minima reveal the boundaries of the crater sources. The horizontal magnetic gradients suggest that the crater is between 12 and 13.5 km in diameter. The low vertical and horizontal magnetic gradients seen at the center of the crater indicate a source about 2.5 km deep, while the high vertical and high horizontal magnetic gradients observed at the edges suggest a relatively shallow source, between 800 m and 2.5 km. The depth computed using flight lines data is in good agreement with the depths from boreholes located close to the crater site (CPRM 1972).

The Euler deconvolution maps (Figs. 4a for $\eta = 2$ and 4b for $\eta = 3$) show estimated source positions and depths. For the gridded magnetic data, the choice of the optimum structural index solutions is based on the standard error of the solutions and tight clustering of the solution. We only accepted depth solutions with relative errors less than 6%. The clustering nature of the Euler solutions with respect to the impact crater anomaly pattern clearly suggests that the solutions are associated with a circular structure buried at shallow depth. The shape of the Serra de Cangalha structure and the structural trends around the crater are shown by the clustering of the solutions around the edge of the crater and on top of the trends. For the circular pattern seen at the center of the map, the depths, computed assuming $\eta = 2$ and 3, are quite close and indicate a magnetic source depth between 1.0 and 1.8 km. These depth values are in good agreement with depths from

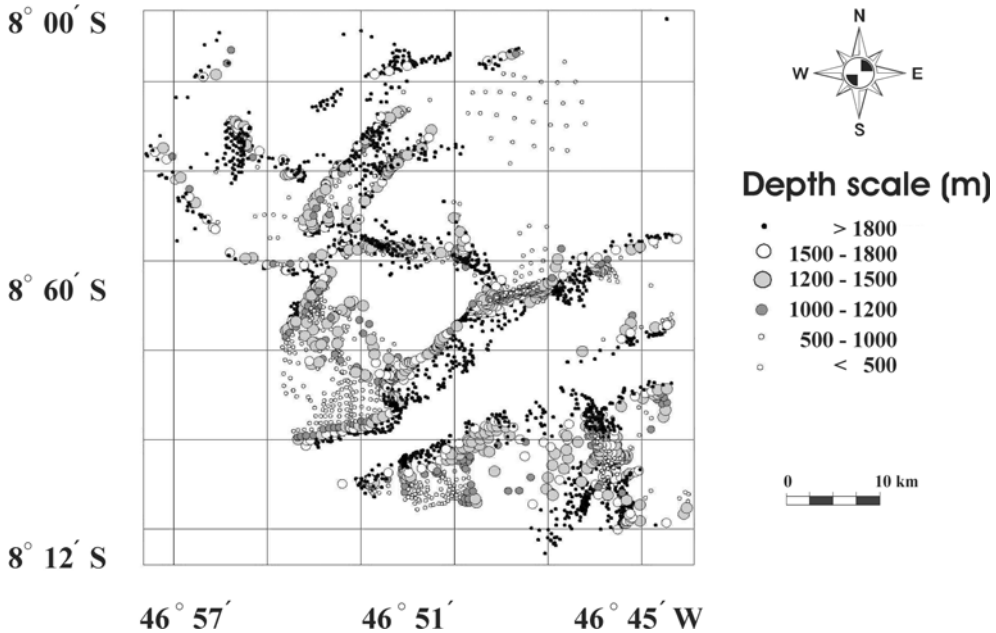

Fig. 4a. Euler depth solutions for $\eta = 2$ for the first vertical derivative of the Serra da Cangalha impact crater aeromagnetic data.

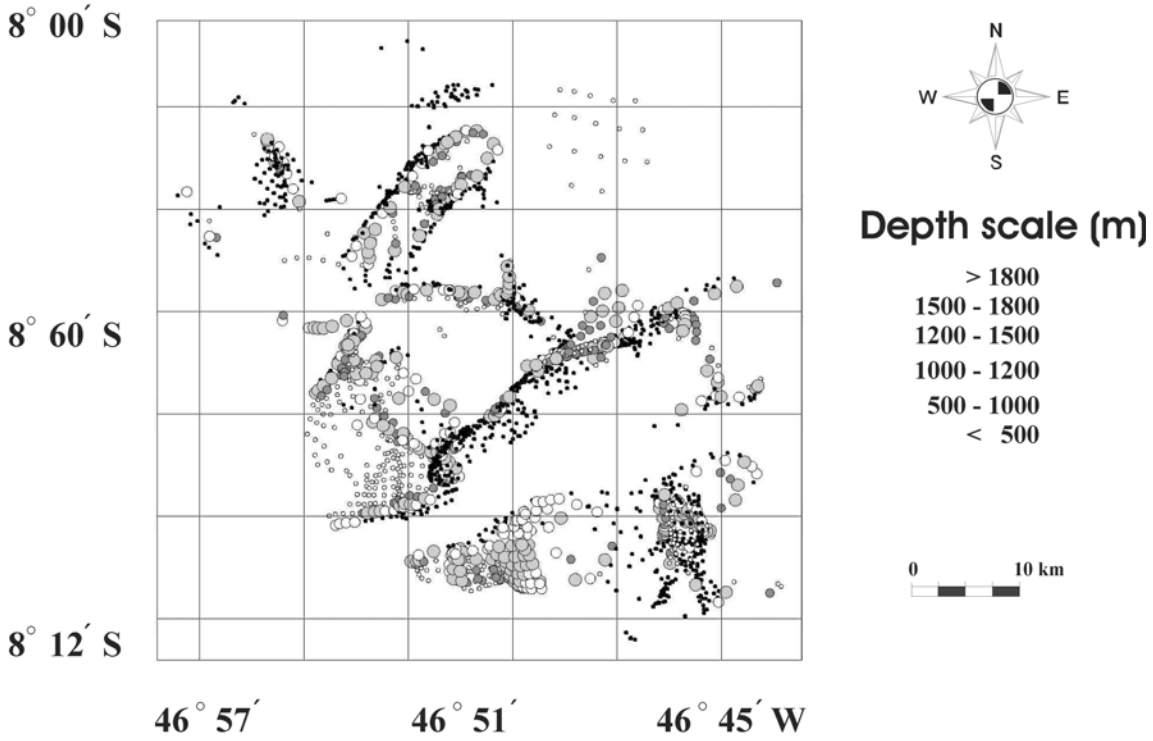

Fig. 4b. Euler depth solutions for $\eta = 3$ for the first vertical derivative of the Serra da Cangalha impact crater aeromagnetic data. The depth information is given by the size of the dots.

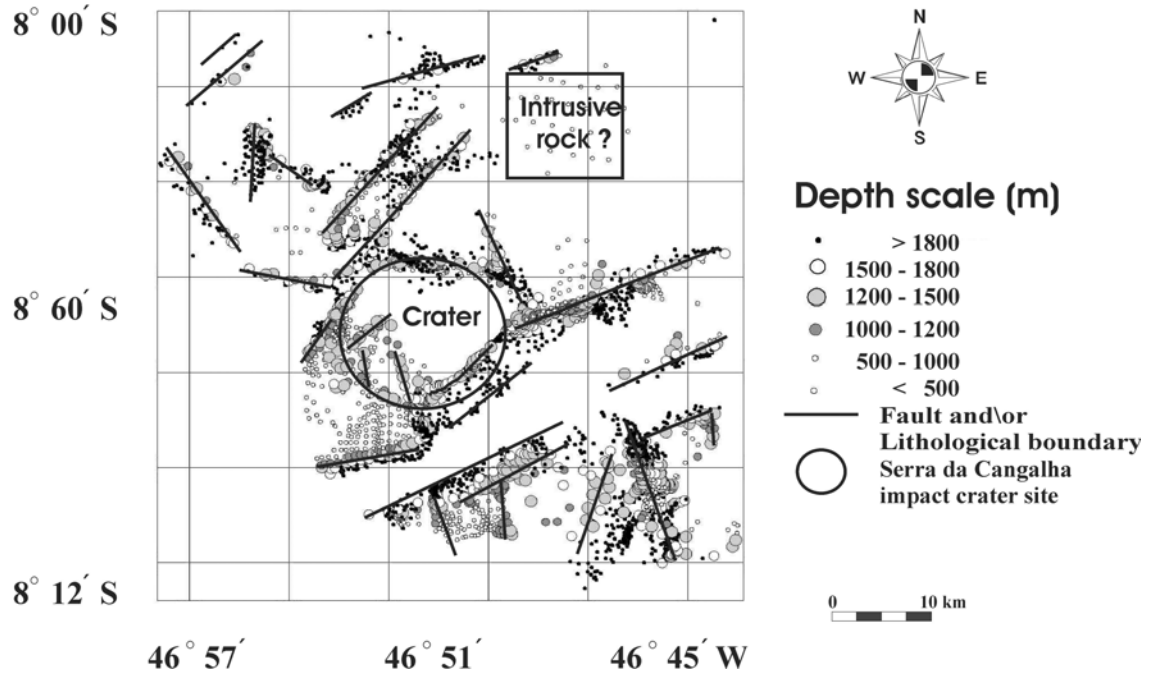

Fig. 4c. Structural interpretation of the Euler solutions for $\eta = 2$.

boreholes located not too far from the crater site, and are coherent with previous studies by Adepelumi et al. (2005).

Figure 4c represents the structural interpretation of the Euler solutions for η = 3 of the gridded data. Two major structural styles are apparent: First, linear features trending NE–SW, ENE–WSW, and NW–SE possibly represent faults and fractures. We are not sure if these features formed pre- or post-impact. Kenkmann and Ivanov (1999) and Morgan et al. (1997) showed that low-angle faulting could result from an impact-induced rheological stratification of the crater floor and passive rotation of the shear zones due to the uplift of the central peak. McHone (1986) and the Geological Survey of Brazil reported compelling evidence that confirmed the existence of structural perturbations of rocks at the crater site. The occurrence of plastic deformations, microfaultings, intense fracturing, brecciated faults, and fragmented impact breccias from the core samples were found to be very common. In general, the dip values of the fault and fracture planes observed in the field range from 45° to 75°. Other lines of evidence include fault plane surfaces that present evidence of striations, polished surface, kink bands in micas, and foliation planes of about 30° to 75°.

The correlation of the location of these structural features to the local geology confirms that these linear features are not an artifact of the Euler deconvolution technique. Second, the magnetic source at the center of the structure has a depth of 1.0 to 1.5 km, corresponding to the Precambrian basement. This result is in agreement with depth estimates obtained from 2-D inversion of the magnetotelluric data by Adepelumi et al. (2005). The Euler solutions are clustered around the edge of the structure, which is a clear indication of the utility of using the Euler technique to delimit the boundary of features in sedimentary terrains.

CONCLUSIONS

The depth estimates and crater shape obtained with the Euler deconvolution method are in good agreement with the estimates from downward continuation of magnetic and magnetotelluric data (Adepelumi et al. 2005). The magnetic fields associated with the central crater anomaly and the associated faults indicate a predominantly shallow source with depth ranging from 1.0 to 1.5 km. The depth solutions clustered around the edge of the crater and on top of the linear features display small standard deviation errors. Based on the theoretical values shown in Table 1, the results suggest that the magnetic structure beneath the crater is close to spherical or may be cylindrical. The crater boundary and size (~12 km in diameter) are defined by maxima and minima of the horizontal and vertical gradients.

Acknowledgments–The Brazilian research council through the CAPES/CNPq scholarship to the first author wholly supported this research. We also acknowledge the Geological Survey of Brazil (CPRM) for making it possible for us to work with the aeromagnetic data. Gordon Cooper and Durrheim of University of Witwatersrand, South Africa are thanked for releasing their 2-D Euler deconvolution software to us free of charge.

Editorial Handling—Dr. Elisabetta Pierazzo

REFERENCES

Adepelumi A. A., Fontes S. L., Schnegg P. A., and Flexor J. M. 2005. An integrated magnetotelluric and aeromagnetic investigation of the structures beneath the Serra da Cangalha impact crater, Brazil. *Physics of Earth and Planetary Science* 150:159–181.

Beatty J. K. 1980. Crater hunting in Brazil. *Sky and Telescope* 59: 464–467.

Cooper G. R. J. 2002. An improved algorithm for the Euler deconvolution of potential field data. *The Leading Edge* 21: 1197–1198.

Crósta A. P. 1987. Impact structures in Brazil. In *Research in terrestrial impact structures*, edited by Pohl J. Wiesbaden: Vieweg & Sons. pp. 30–38.

Dietz R S. and French B. M. 1973. Two probable astroblemes in Brazil. *Nature* 244:561–562.

Durrheim R. J. and Cooper G. R. J. 1998. Euldep, a program for the Euler deconvolution of magnetic and gravity data. *Computers and Geosciences* 24:545–550.

Geological survey of Brazil (CPRM). 1972. Report of the research on industrial diamond in the region of Serra da Cangalha, Goias State. pp. 1–17.

Góes A M. O. and Feijó F. J. 1994. Bacia do Parnaíba. *Boletim Geociências da Petrobrás* 8:57–67.

Grauch V. J. S. and Cordell L. 1987. Limitations of determining density or magnetic boundaries from the horizontal gradient of gravity or pseudogravity data. *Geophysics* 52:118–121.

Grieve R. A. F. 1990. Impact cratering on the Earth. *Scientific American* 262:66–73.

Gunn P. J. 1975. Linear transformations of gravity and magnetic fields. *Geophysical Prospecting* 23:300–312.

Hsu S. K. 2002. Imaging magnetic sources using Euler's equation. *Geophysical Prospecting* 50:15–25.

Keating P. 1998. Weighted Euler deconvolution of gravity data. *Geophysics* 63:1595–1603.

Keating P. and Pilkington M. 2004. Euler deconvolution of the analytical signal and its application to magnetic interpretation. *Geophysical Prospecting* 52:165–182.

Kenkmann B. and Ivanov A. 1999. Low-angle faulting in the basement of complex impact craters: Numerical modeling and field observations in the Rochechouart structure, France (abstract #1544). Proceedings, 30th Lunar and Planetary Science Conference. CD-ROM.

McHone J. F. 1986. Terrestrial impact structures: Their detection and verification with new examples from Brazil. Ph.D. thesis, University of Illinois at Urbana-Champaign, Urbana, Illinois, USA. 210 p.

Morgan J. O., Warner M., The Chicxulub Working Group, Britain J., Buffler R., Camargo A., Christeson G., Denton P., Hildebrand A., Hobbs R., Macintyre H., Mackenzie G., Maguire P., Marin L., Nakamura Y., Pilkkington M., Sharpton V., Snyder D., Suarez G., and Trejo A. 1997. Size and morphology of the Chicxulub impact crater. *Nature* 390:472–476.

Mushayandebvu M. F., Lesur V., Reid A. B., and Fairhead J. D. 2004.

Grid Euler deconvolution with constraints for 2D structures. *Geophysics* 69:489–496.

Pilkington M. and Grieve R. A. F. 1992. The geophysical signature of terrestrial impact craters. *Reviews of Geophysics* 30:161–181.

Ravat D., Wang B., Wildermuth E., and Taylor P. T. 2002a. Gradients in the interpretation of satellite-altitude magnetic data: An example from central Africa. *Journal of Geodynamics* 33:131–142.

Ravat D., Kirkham K., and Hildenbrand T. G. 2002b. A source-depth separation filter: Using the Euler method on the derivatives of total intensity magnetic anomaly data. *The Leading Edge* 21: 360–365.

Reid A. B., Allsop J. M., Granser H., Millett A. J., and Somerton I. W. 1990. Magnetic interpretation in three dimensions using Euler deconvolution. *Geophysics* 55:80–91.

Tappan H. 1982. Extinction or survival: Selectivity and causes of Phanerozoic crises. In *Geological implications of impacts of large asteroids and comets on the earth*, edited by Silver L. T. and Schultz P. H. Special Paper #190. Boulder: Geological Society of America. pp. 265–276.

Thompson D. T. 1982. EULDPH—A new technique for making computer-assisted depth estimates from magnetic data. *Geophysics* 47:31–37.